# An application of Ti-K X-ray absorption edges and fine structures to the study of substoichiometric titanium carbide TiC1-x

V. Moisy-Maurice, C.H. de Novion

*J. Phys. France* **49** (1988) 1737-1751 OCTOBRE **1988,** PAGE 1737

Classification
*Physics Abstracts*
78.70D — 61.70B

# An application of Ti-K X-ray absorption edges and fine structures to the study of substoichiometric titanium carbide $TiC_{1-x}$

V. Moisy-Maurice and C. H. de Novion

C.E.A./IRDI/DMECN/DTech, Laboratoire des Solides Irradiés, Ecole Polytechnique, 91128 Palaiseau Cedex, France

(*Reçu le 21 janvier 1988, accepté sous forme définitive le 9 juin 1988*)

**Résumé.** — Des mesures à haute résolution du coefficient d'absorption de rayons X ont été effectuées au voisinage de et jusqu'à 1 000 eV au-dessus du seuil K du titane dans des échantillons de $TiC_{1-x}$, $(0{,}5 \leqslant 1-x \leqslant 0{,}97)$. Quand la teneur $x$ en lacunes de carbone augmente, (i) la charge effective positive du titane déduite de l'énergie du seuil diminue, (ii) le bas des bandes 4p du titane (situé à 10-15 eV au-dessus du niveau de Fermi $E_F$ dans $TiC_{0,97}$) se déplace progressivement en direction de $E_F$. A partir de l'amortissement des oscillations d'Exafs qui augmente avec l'écart à la stœchiométrie, les déplacements relatifs statiques quadratiques moyens des premiers voisins titane-titane et titane-carbone ont été évalués. Un modèle simple où toute lacune de carbone repousse ses premiers voisins titane de 0,08 Å est proposé.

**Abstract.** — High-resolution measurements of the X-ray absorption coefficient were made around and up to 1 000 eV above the titanium K-edge of $TiC_{1-x}$ samples $(0.5 \leqslant 1-x \leqslant 0.97)$. When increasing the carbon vacancy content $x$, (i) the positive effective charge of titanium deduced from the edge-shift decreases, (ii) the bottom of the titanium 4p bands (situated at 10-15 eV above the Fermi level $E_F$ in $TiC_{0.97}$) moves down progressively towards $E_F$. From the increased damping of the Exafs oscillations with non-stoichiometry, average mean-square static relative displacements of titanium-titanium and titanium-carbon first neighbours are evaluated. A simple model where each carbon vacancy repells its first neighbours Ti by 0.08 Å is proposed.

## 1. Introduction.

Beyond their numerous remarkable physical properties, cubic rocksalt transition metal carbides present a large domain of existence. For example, titanium monocarbide can accommodate up to $\simeq 50$ % vacancies in the carbon sublattice, so that the $TiC_{1-x}$ phase extends from $TiC_{0.97}$ to $TiC_{0.50}$ [1]. The influence of vacancy concentration on the bulk physical properties of the carbides has been extensively studied [2] ; but a detailed atomic and electronic description of non-stoichiometry is still lacking [3], although recently a qualitative understanding of the ordering of carbon vacancies has been undertaken from the calculation of « first principle » pair potentials [4].

The extended X-ray absorption fine structure (Exafs) consists of the oscillations of the absorption coefficient that occur up to 1 500 eV above an edge in condensed materials. Exafs data can give information about the number, kind and distance of atoms surrounding a given one, and the damping of the oscillations when the incident photon energy increases is partially due to thermal and static disorder effects (for a review, see [5]). Furthermore, the absorption edges themselves are strongly related to the partial local electronic densities of states of the absorbing compound.

A detailed study of the titanium K X-ray absorption spectrum in stoichiometric TiC has been made by Balzarotti *et al.* [6]. In this paper, we present systematic measurements of the absorption coefficient of $TiC_{1-x}$ around the TiK-edge. The evolution with $1-x$ of the near-edge structure (Xanes) — situated in the 30 eV following the threshold — has been analysed, and it has been possible to deduce from the Exafs oscillations large mean square static displacements of the Ti atoms in the non-stoichiometric compounds.

## 2. Experimental.

2.1 SAMPLES. — $TiC_{1-x}$ powder samples ($1-x$ = 0.97, 0.9, 0.8, 0.7, 0.6, 0.5) were prepared by pressing and sintering at 1 500 °C mixtures of titanium hydride $TiH_2$ and graphite as described in [7]. Their characteristics are listed in table I. The measured lattice parameters $a(x)$ (determined by X-ray diffraction) are in good agreement with literature values [1] ; the main metallic impurities, analysed in the $TiC_{0.7}$ sample, are in p.p.m. weight : V 150, Al 70, Fe 40, Si 35 and Cr 20.

Table I. — *Characteristics of* $TiC_{1-x}$ *samples.*

| « Nominal » composition | Measured lattice parameter ($10^{-10}$ m) | Measured C/Ti atomic ratio | Oxygen (ppm weight) | Nitrogen (ppm weight) |
|---|---|---|---|---|
| $TiC_{1.0}$ | 4.3283 (8) | $\simeq 0.97$ | 1 530 | — |
| $TiC_{0.9}$ | 4.3302 (8) | 0.895 | 1 260 | 1 680 |
| $TiC_{0.8}$ | 4.3292 (8) | — | — | — |
| $TiC_{0.7}$ | 4.3242 (8) | 0.687 | 1 600 | 1 060 |
| $TiC_{0.6}$ | 4.3162 (8) | — | — | — |
| $TiC_{0.5}$ | 4.3067 (30) | 0.51 (*) | — | — |

(*) In $TiC_{0.5}$, the presence of 2 % residual Ti metal was observed and the homogeneity of the sample was not so good as for other compositions.

As the X-ray absorption coefficient measurements require thin ($\simeq$ 10 μm for TiC) and homogeneous samples, the compounds have been carefully ground before being fixed between adhesive foils. The absence of holes and constance of thickness have been checked by optical microscopy.

2.2 ABSORPTION COEFFICIENT MEASUREMENTS. — They were made on the Exafs spectrometer 1 at L.U.R.E. (Orsay, France), using the synchrotron radiation of the collision ring D.C.I. This apparatus allows to record X-ray absorption coefficient data in the 3-15 keV range of photon energy, i.e. wavelengths between 0.4 and 0.08 nm [8]. The monochromator was Si (220) channel-cut, with a resolution of 1.2 eV at 5 keV. A helium gas cryostat with mylar windows was used to perform measurements at 10 K, with a stability of ± 2 K. The experimental technique is described in detail elsewhere [9].

## 3. Results.

Two kinds of experiments were performed.

(a) A precise study at 300 K of the Ti-K absorption edges (Xanes) : the X-ray absorption coefficient $\mu(E)$ was measured every 0.1 eV on a 50 eV energy range around the threshold. The absorption coefficient of (quasi-) stoichiometric « TiC » (i.e. $TiC_{0.97}$) shows a complex energy dependence, already observed previously [6] : in particular, a first small step at the threshold and a large increase around 15 eV above. This general aspect remains in non-stoichiometric $TiC_{1-x}$, although the step height at the threshold increases and the shape evolves towards the pure Ti one (see Fig. 1).

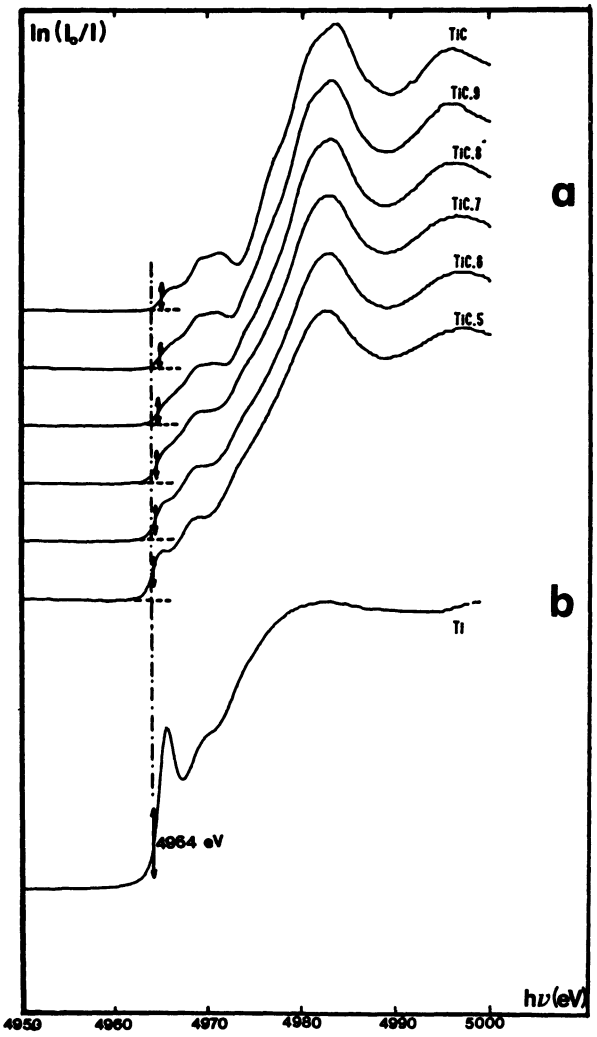


Fig. 1. — X-ray K-absorption edges for titanium atoms : (a) in $TiC_{1-x}$ ; (b) in Ti metal.

In order to be able to compare quantitatively the positions of the edges, it was necessary to make an accurate calibration of the incident photon energies before and after each measurement : the reference used was the maximum of the narrow peak located at 4 965.5 eV in the beginning of the pure Ti metal spectrum (Fig. 1b). A global shift of the edges towards high energies is clearly visible from Ti to « TiC ».

(b) The Exafs oscillations $\chi(E)$ were studied at 10 and 300 K : the X-ray absorption coefficient data were recorded every 1.5 eV from 500 eV below to 1 000 eV above the Ti-K edge. The aim of the low temperature experiments was to get rid of a great part of the thermal damping effects on Exafs oscillations. In figure 2 are compared the Exafs spectra of « TiC » and $TiC_{0.7}$ at 10 K, after separation from background and normalization (for details, see [9]) : the oscillations are similar for the two compounds, but an important additional damping occurs for the substoichiometric sample, that we attribute to its high defect concentration.

## 4. Absorption edges : discussion.

4.1 « STOICHIOMETRIC » TiC. — The $\mu(E)$ variation just above the titanium K-edge (Xanes) shows several features displayed in figure 3a, and which are, at increasing incident photon energy :

— the threshold (labelled A), chosen as the inflexion point at the first step ;

— two small maxima (B and C) respectively at 3.5 and 6.5 eV above A ;

— a large increase between 8 and 15 eV, with a small shoulder (D) around 12.5 eV ;

— two strong maxima (E and F) at 18.7 and 30.6 eV.

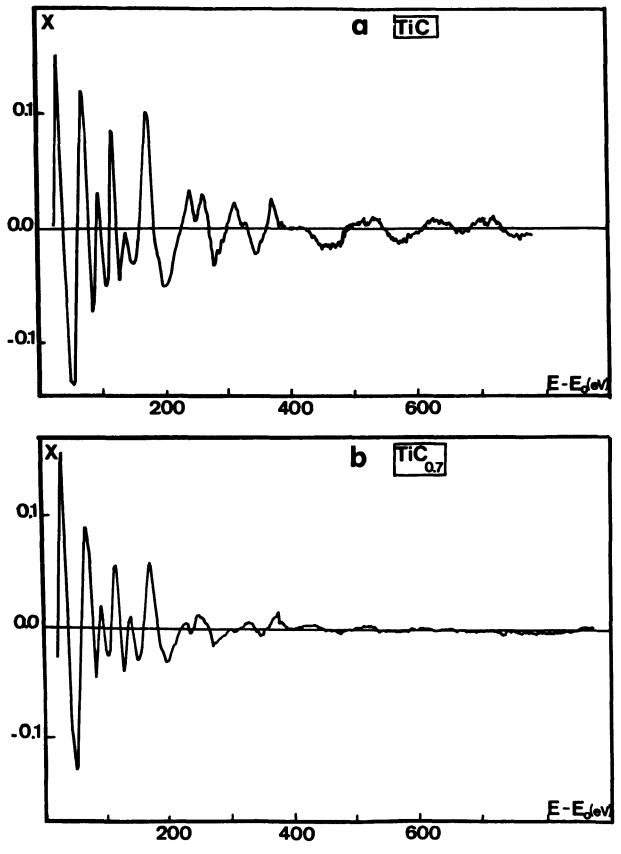


Fig. 2. — Exafs spectra measured at 10 K at the titanium K-edge : (a) in TiC ; (b) in $TiC_{0.7}$.

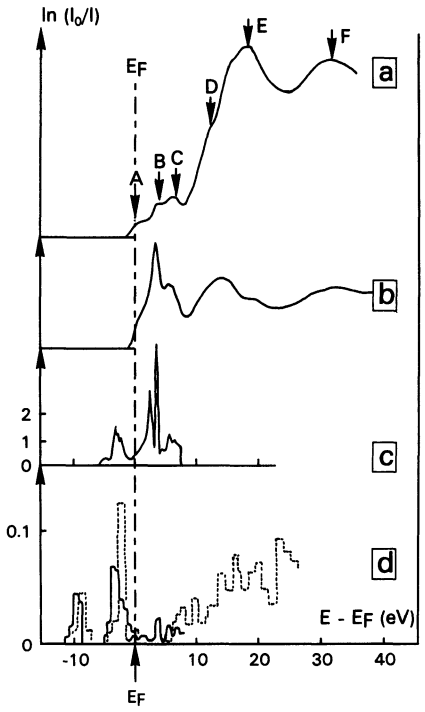


Fig. 3. — Titanium and carbon K absorption near-edge structures in TiC compared to band structure calculations. (a) Experimental results for Ti (present work) ; (b) Experimental results for C (Ref. [11]) ; (c) Partial local density of states $N_d^{Ti}(E)$ deduced from APW calculations (Ref. [15]) ; (d) Partial metal p density of states deduced from APW calculations on TiC ($N_P^{Ti}(E)$, full line, from Ref. [12]), and on NbC ($N_P^{Nb}(E)$, dotted line, shifted in energy from the data of reference [14] to fit $E_F$(TiC)).

It is generally agreed now that in metallic systems, where screening of the core hole by the final state electrons is effective, the Xanes spectra are well interpreted within a band structure approach (i.e. many-body effects can be neglected). Indeed, it has been shown by Müller *et al.* [10], that for pure metals (including Ti), the $\mu(E)$ variation in the 100 eV above the threshold is well explained by a one-electron approximation ; in the case of K edges, it is in good agreement with the p partial density of states multiplied by the appropriate (dipolar) transition probability and convoluted by an energy-

dependent broadening function due to lifetimes of the core hole and of the excited electron. Also, in VN (which is similar in crystal structure and type of bonding to TiC), the nitrogen K near-edge structure follows the shape of the total density of states up to 40 eV above the Fermi level $E_F$ [11].

Therefore, we have reported in figures 3c and 3d the available partial d and p densities of states localized on the metal atom : $N_d^{Ti}(E)$, $N_p^{Ti}(E)$ (up to 8 eV above $E_F$) and $N_p^{Nb}(E)$, calculated for TiC [12, 13] and NbC [14] respectively. One can see that in TiC the titanium p density of states is very weak in the 8 eV above the Fermi level, and that the bottom of the metal 4p band is situated at 10-15 eV above $E_F$.

The experimental results of figure 3a compared to the calculated densities of states of figures 3c and 3d suggest the following independent electron interpretation, already proposed by Balzarotti *et al.* [6], assuming the threshold A is due to transitions from the 1s core to the Fermi level $E_F$ :

— peaks B and C (barely seen on $N_p^{Ti}(E)$) correspond precisely to the metal 3d density of states maxima calculated by Neckel *et al.* [15] : 3.5 and 6.2 eV above $E_F$ for the 3d $t_{2g}$ and 3d $e_g$ bands respectively ;

— the large increase of $\mu(E)$ between 10 and 20 eV above the threshold, and peak E, correspond to the titanium 4p bands ;

— shoulder D is possibly due to the Ti 4s band.

This interpretation, in qualitative agreement with the molecular orbital approach of Fischer [16], is confirmed by other experiments :

— peaks B, C and E were observed for TiC by Bremsstrahlung Isochromat Spectroscopy, which also probes the vacant electronic states [17] ;

— peaks at similar positions, but with different relative intensities, were observed on the $\mu(E)$ curve above the K-*carbon* edge for TiC [11] (see Fig. 3b) : at 3.6 eV above $E_F$ ($\equiv$ B, but very sharp), at 6.2 eV ($\equiv$ C), at 14.4 eV ($\simeq$ D ?), at 23 and 33 eV ($\simeq$ E and F respectively, but very weak). On the basis of the density of states calculation for VN cited above, they were attributed respectively to 3d $t_{2g}$ (for B), 3d $e_g$ (for C), 4s (for D) and 4p (for E and F) metal states hybridized with the 2p-3s-3p metalloid states [11].

One may remark that the Ti-K Xanes in TiC has striking similarities with that in $TiO_2$ [18], with low intensity absorption features (corresponding to transitions to 3d levels or narrow bands) preceeding the onset of the main absorption peak due to the dipolar $1s \rightarrow 4p$ transition. Although TiC is metallic and $TiO_2$ is a 3 eV gap semi-conductor, the similarity of their absorption spectra is due to (i) the absence of metal p states in the 10 eV above the Fermi level, (ii) the similar metalloid environments of Ti atoms (regular octahedra in TiC, slightly distorted octahedra in $TiO_2$), (iii) the absence of excited states multiplet splitting in $TiO_2$ because the ground state configuration is $3d^\circ$, (iv) the similar formal valence (4 +) of Ti in the two compounds.

In stoichiometric TiC, where Ti is surrounded by a regular carbon octahedron ($O_h$ symmetry), $1s \rightarrow 3d$ transitions are forbidden in the usual dipolar approximation. Therefore, the low value of the ratio $N_p^{Ti}(E)/N_d^{Ti}(E)$ ($\lesssim 10^{-2}$ in the 2-5 eV range above $E_F$ in TiC), and the coincidence of B and C maxima with those of the 3d band density of states, suggest that these maxima are due to quadrupolar transitions. (In transition metals, where $N_p$ and $N_d$ are comparable, the quadrupolar contribution to $\mu$ near the K edge is a few percent of the dipolar [19]).

The Ti-K edge-shift, measured as the change of position of the first inflexion point in the $\mu(E)$ curve between TiC (point A) and Ti, was found equal to : $\Delta E_K(TiC) = E_K(TiC) - E_K(Ti) = 1.1 \pm 0.2$ eV, in good agreement with previous X-ray absorption determinations ($0.7 \pm 0.4$ eV [20], $\sim 1$ eV [6]). For metallic compounds such as TiC, there is no available empirical model allowing to deduce directly from $\Delta E_K$ an effective charge or a coordination charge as has been done for oxides [21]. However, as the variation of $E_F$ between Ti and TiC is suggested to be less than 0.2 eV from thermoionic work function measurements [22], and screening seems to be effective in both compounds at low photoelectron energy [6], a « naive » model will attribute the chemical shift mainly to a larger 1s core level binding energy in TiC than in Ti, due to a charge transfer from titanium to carbon atoms ; this is in qualitative agreement with APW band calculations (charge transfer : $\simeq 0.4$ electron in TiC) and with the overall spectroscopic properties [20, 23].

It may be remarked that $\Delta E_K(TiC)$ is found close to the XPS Ti 1s chemical shift : $1.0 \pm 0.4$ eV [20], $0.8 \pm 0.1$ eV [22], whereas the Ti-L emission and absorption edge differs from the L-XPS edge by $\simeq 1.5$ eV. The latter fact was attributed to incomplete screening of the suddenly created XPS Ti-2p hole in TiC, due to the low density of states at the Fermi level [6] and suggests that many-body effects are more easily observed for L than for K metal atom edges in this compound.

**4.2** SUBSTOICHIOMETRIC $TiC_{1-x}$. — With increasing non-stoichiometry, the titanium K Xanes in $TiC_{1-x}$ is progressively modified.

**4.2.1** The value of the absorption coefficient at the edge (point A) increases with vacancy concentration. One indeed observes a correlated increase of the electronic density of states at the Fermi level $N(E_F)$ from low temperature specific heat measurements [24].

Theoretical density of states calculations (for disordered $TiC_{1-x}$ modelized by CPA [25, 26] and hypothetically ordered $TiC_{0.75}$ [13, 27]), X-ray emission measurements [28] and $^{13}C$ N.M.R. measurements on the isomorphous compound $ThC_{0.75}$ [29], show that this increase corresponds to states originating from metal d orbitals. Therefore, the $\mu(E_F)$ increase with $x$ must be explained by quadrupolar transitions (as proposed above for the B and C peaks in stoichiometric TiC), or by 3d-4p hybridization induced by vacancies, as suggested by molecular orbital calculations [28]. The fact that the height of the first step at the carbon K-edge does not change with composition [11] shows that the metal d states involved in the increase of $N(E_F)$ with $x$ are not hybridized with carbon 2p states (dangling bonds).

4.2.2 The overall edge and near-edge structure is shifted towards low energies with increasing vacancy concentration $x$. In particular, the edge-shift at the threshold $\Delta E_K(TiC_{1-x})$ decreases linearly with $x$ (see Fig. 4) and we extrapolate a zero value near the composition $TiC_{0.4}$.

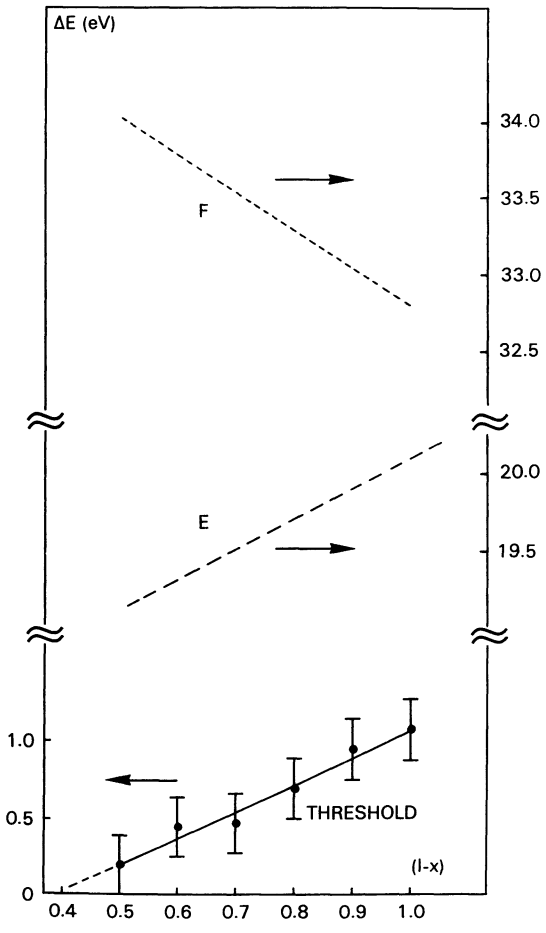


Fig. 4. — Titanium K-absorption edge shift from Ti metal to $TiC_{1-x}$ measured at the threshold (point A) (——, ⊕). For comparison are plotted the shifts measured at the $\mu(E)$ maxima (point E : (------), and F : (.....)).

A similar behaviour was observed in XPS studies of $Ti_{2p\,3/2}$ level shifts [22, 30]. As the Fermi level change in the homogeneity range of $TiC_{1-x}$ is less than 0.3 eV, as shown by the $x$ independent carbon K edge-shift measured by electron loss spectroscopy [11] and the most recent CPA [26] and band [13, 27] calculations, the decrease of $\Delta E_K$ and $\Delta E_{2p\,3/2}$ can be related to a change with composition of the positive effective charge on the metal atoms. Up to now, theoretical studies disagree on this point : cluster calculations suggest a decrease of the effective charge of titanium atoms adjacent to vacancies [28] ; on the other hand, recent theoretical APW calculations for a long-range ordered $TiC_{0.75}$ crystal, find practically the same titanium effective charge as in TiC [13, 27] ; the discrepancy might be due to the ordered structure chosen by the latter authors, with two carbon vacancies disposed symmetrically around titanium atoms, in contradiction with experiment [3].

4.2.3 The main increase of $\mu(E)$ (between points C and E) occurs in a broader energy range with increasing $x$, and progressively merges into the low energy structures (the C maximum disappears for $1 - x \leqslant 0.7$) : the bottom of the metal 4p bands moves down towards the Fermi level in proportion as the repulsion by carbon 2s states decreases. This is in agreement with the calculations of Zhukov and Gubanov [13] which show that in $TiC_{0.75}$ the bottom of the 4p Ti band is around 9 eV above $E_F$, and a first peak of density of states $N_p^{Ti}(E)$ occurs at + 11.5 eV (which is seen as a shoulder on the absorption spectrum of $TiC_{0.7}$, see Fig. 1).

4.2.4 The second maximum of $\mu(E)$, F, is found to shift at higher energies with increasing non-stoichiometry ( + 1.3 eV from TiC to $TiC_{0.5}$, see Fig. 4). Theoretical cluster calculations for the isomorphous compound $VO_x$ [31] have shown that this second maximum F is mainly due to scattering of the photoelectron by the first metalloid neighbours (at 30 eV, the photoelectron mean free path $\lambda$ is only $\simeq 5$ Å), and is very sensitive to the interatomic distance $\bar{R}$ between metal and metalloid. We have applied the Natoli [32] relation $\overline{R_{Ti\text{-}C}}\sqrt{E - E_{ref}} =$ Cte to the $TiC_{1-x}$ solid solution with $E_{ref}$ taken as the muffin-tin zero of the calculated band structure (9.0 eV below the Fermi level in TiC [15]), $E$ position of the maximum F, and $\overline{R_{Ti\text{-}C}}$ average Ti-C first neighbour distance. For small changes $\Delta E$ and $\Delta\overline{R_{Ti\text{-}C}}$, this leads to a linear relationship $\Delta\overline{R_{Ti\text{-}C}} \simeq -\dfrac{\overline{R_{Ti\text{-}C}}}{2(E - E_{ref})}\Delta(E - E_{ref})$. From the data of figure 4, $\Delta(E - E_{ref})$ (eV) = $(2.5 \pm 0.4)x$ if $E_{ref}$ is kept constant with $x$. This leads to an average contraction of the Ti-C first neighbour distance in $TiC_{1-x}$ relative to TiC : $\Delta\overline{R_{Ti\text{-}C}}$(Å) = (− 0.065 ±

0.02) $x$ (the error bar includes an uncertainty of $\pm 5$ eV on $E_{ref}$). This relation between ligand compression and shift of peak F is in qualitative agreement with the cluster calculations on $VO_x$ [31]. The change of $\overline{R_{Ti\text{-}C}}$ with $x$ will be compared to the Exafs results in a following paragraph.

## 5. Exafs : analysis and discussion.

5.1 DATA ANALYSIS. — The equation for the Exafs function in a spherically averaged moderately disordered system, assuming no multiple scattering, is given by [5] :

$$\chi(k) = \sum_j \chi_j(k) \simeq - \sum_j \frac{N_j}{k\overline{R_j^2}} |f_j(k, \pi)| \, e^{-2\bar{R}_j/\lambda(k)} \times \int_0^\infty g(R_j) \sin(2kR_j + \psi_j(k)) \, dr_j \quad (1)$$

— $k$ is the wave-vector of the ejected photoelectron ;

— $\chi_j$ is the Exafs contribution of the $j$-th shell of neighbours containing $N_j$ atoms of back-scattering amplitude $f_j(k, \pi)$ and situated at an average distance $\overline{R_j}$ of the central absorbing atom ;

— $\psi_j(k)$ is the $k$ dependent photoelectron phase-shift resulting from the central and back-scattering atoms ; it is usually a quasi-linear decreasing function of $k$ : $\psi_j \simeq \beta_j - \alpha_j k$ (2) (see Fig. 6) ;

— the damping of the spectrum due to the photoelectron life-time is represented by the term $e^{-2\overline{R_j}/\lambda(k)}$, where $\lambda$ is of the order of 5 to 20 Å ;

— the effect of atomic disorder is represented by the radial distribution function $g(R_j)$ of the distance $R_j$ between the central atom and the $j$-th neighbour shell atoms ; in the moderately disordered systems considered, its width is small relatively to the interatomic distance ; it takes into account thermal vibrations and static displacements ; in the case of the harmonic approximation (small thermal vibrations), $g(R_j)$ is a Gaussian function, and the integral in equation (1) can be replaced by :

$$e^{-2\sigma_j^2 k^2} \sin(2k\overline{R_j} + \psi_j(k)) \quad (3)$$

where $\sigma_j^2$ is the mean-square relative displacement between the central atom and its $j$-th surrounding shell ; yet, this Debye-Waller type approximation is generally not valid for statically disordered materials.

The wave-vector $k$ of the ejected photoelectron, which may be considered as free when its kinetic energy $E$ exceeds 50 eV, is given by the equation $\hbar^2 k^2/2 m_e = E - E_0$, where $m_e$ is the electron mass and $E_0$ a « zero potential ». In fact, because of the complex shape of the near-edge structure, there is no way to determine experimentally $E_0$ (within a few eV) ; the problem of the choice of $E_0$ has been largely discussed in literature, and it is generally agreed to make it an adjustable parameter in the analysis [5]. In our case, $E_0$ was taken for all samples as the edge energy determined in section 4 : this choice optimized the $k$-independency of interatomic distances $\bar{R}_j(k)$ determined from the Exafs data ($\pm 0.015$ Å for the first Ti-Ti neighbours in $TiC_{0.8}$ for $3 < k < 11$ Å$^{-1}$). It is important to note that a 2 eV variation of $E_0$ for a given phase-shift $\psi_j(k)$ introduces a 0.01 Å change of the interatomic distance $\bar{R}_j$.

Our Exafs data were analysed by back-Fourier transform filtering ; the Fourier transformation used was :

$$\text{F.T. } (k^3 \chi(k)) = \int_{-\infty}^{+\infty} k^3 \chi(k) \, e^{2ikR} \, W(k) \, dk$$

where $k^3$ is a multiplicative term introduced in order to amplify the high $k$ Exafs oscillations ; $W(k)$ is an apodized rectangular window function, the extremities of which are $k_{min} = 2$ Å$^{-1}$ (lower validity limit

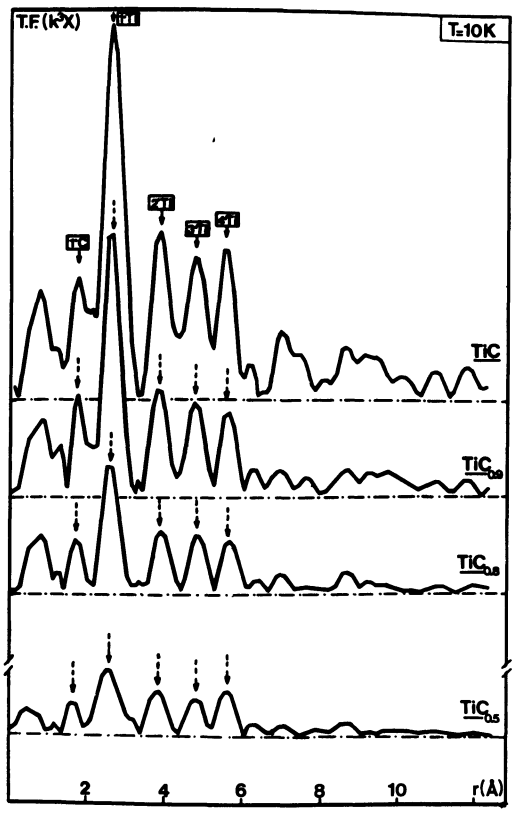


Fig. 5. — Fourier transform magnitude $|\text{F.T. } (k^3 \chi(k))|$ of $TiC_{1-x}$ Exafs spectra measured at 10 K. The arrows indicate the positions of near neighbour shells, assuming a constant $\alpha_j = 0.86$ Å.

of the Exafs formula (1)) and $k_{max} = 12$ Å$^{-1}$ (higher limit of recorded data) [9].

It can be seen in figure 5 that the near neighbour shells contribute to the F.T. magnitude by peaks situated approximately at distances $\bar{R}'_j = \bar{R}_j - \alpha_j/2$, $\alpha_j$ (the slope of $\psi_j$ *versus-k*) being close to 0.86 Å. In fact, because of the weak backscattering amplitude of carbon, only the first neighbour carbon shell is observed. The intensity of the titanium peaks decreases with the distance of the shell, which is due to the various damping factors in formula (1). At last, an increase of temperature or of carbon vacancy content results in a damping of the Fourier transform.

Then, inverse Fourier transformation applied to each of these peaks allows to isolate the different atomic shell contributions $\chi_j(k)$ to the Exafs, and to analyse them separately.

In the case of stoichiometric TiC, where the interatomic distances $\bar{R}_j$ are precisely known, the phase shift $\psi_j(k)$ for each shell $j$ of neighbours could be experimentally determined from the zeros of the filtered $\chi_j(k)$ function (see Fig. 6). For Ti-Ti and Ti-C first neighbours, the $\psi_j(k)$ curves are in good agreement with those obtained by Balzarotti *et al.* [6] ; these authors explained the difference with the ionic phase-shifts calculated by Teo and Lee [33] (difference which can be partly corrected by a shift of $E_0$, $\Delta E_0 \simeq 8$ eV), in terms of the dynamical screening model developed by Noguera and Spanjaard [34]. At last, we attribute the large difference between the 2nd and 4th Ti-Ti neighbour phase-shifts and those of the other shells, to collinear multiple scattering, as these atoms are separated from the central atom by C and Ti first neighbours respectively.

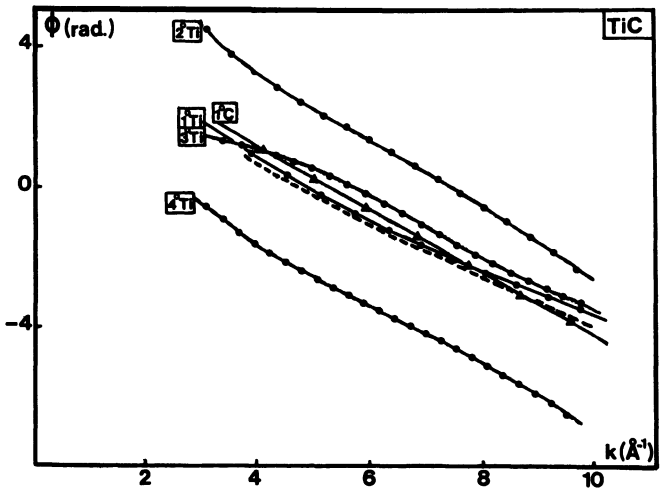


Fig. 6. — Experimental total phase-shifts (backscattering + twice central) with zero potential $E_0$ situated at the absorption edge, for the neighbour shells of a central Ti in TiC (first carbon shell, four first titanium shells). The phase-shift for the first Ti neighbours in pure titanium has been added for comparison (dotted line).

5.2 INTERPRETATION BY THE CLASSICAL GAUSSIAN MODEL OF DISORDER. — In such a model, for each neighbour shell $j$ of the central absorbing atom, formula (1) reduces to :

$$\chi_j(k) \simeq -\frac{N_j}{k\bar{R}_j^2} |f_j(k, \pi)| \, e^{-2\bar{R}_j/\lambda(k)} \times \times e^{-2\sigma_j^2 k^2} \sin(2k\bar{R}_j + \psi_j(k)) \quad (4)$$

where the static and thermal disorder effects are weak and uncorrelated : $\sigma_j^2 = \sigma_{j\,\text{stat.}}^2 + \sigma_{j\,\text{therm.}}^2$. It is in a first stage assumed that $\psi_j(k)$, $\lambda(k)$, $|f_j(k, \pi)|$ remain independent of temperature and composition in $TiC_{1-x}$.

The analysis of partial Exafs contributions $\chi_j(k)$ was mainly restricted to the two first neighbour shells (Ti-C and Ti-Ti), the contributions of more distant shells being complicated by multiple scattering effects ; because of the poor $\chi_{\text{Ti-C}}(k)$ signal, the uncertainties on crystallographic data obtained for the first neighbour Ti-C shell are rather large.

5.2.1 *Mean interatomic distances.* — The $\bar{R}_j$ dependence with $x$ was deduced from the zeros of $\chi_j(k)$ at 10 K (using $\psi_j(k)$ determined in TiC, as described Sect. 5.1) ; it is represented in figure 7 for the first neighbours Ti-C and Ti-Ti in comparison with the corresponding distances deduced from the lattice parameter : $a(x)/2$ and $a(x)\sqrt{2}/2$ respectively.

In the case of the Ti-Ti first neighbours, the average distance should remain equal to $a(x)\sqrt{2}/2$ because the Ti sublattice is totally occupied [35] ; the apparent contraction of $\overline{R_{\text{Ti-Ti}}}$ (compared to $a(x)\sqrt{2}/2$) could not be suppressed by using Ti phase-shifts interpolated between those of TiC and Ti pure metal (see Fig. 7). Similar conclusions could be drawn for the Ti-Ti second, third and fourth neighbour shells.

5.2.2 *Thermal vibrations.* — Information on $\sigma_{j\,\text{therm.}}^2$ is obtained from the amplitude ratio of the partial Exafs functions of a given compound at 10 and 300 K :

$$\frac{1}{2}\ln\left[\frac{\chi_{j\,10\,\text{K}}(k)}{\chi_{j\,300\,\text{K}}(k)}\right] = (\sigma_j^2(300\,\text{K}) - \sigma_j^2(10\,\text{K}))\,k^2 . \quad (5)$$

In figure 8, it is seen that for the Ti-Ti and Ti-C first neighbour shells in TiC, relation (5) is obeyed, i.e. that the harmonic approximation describes well

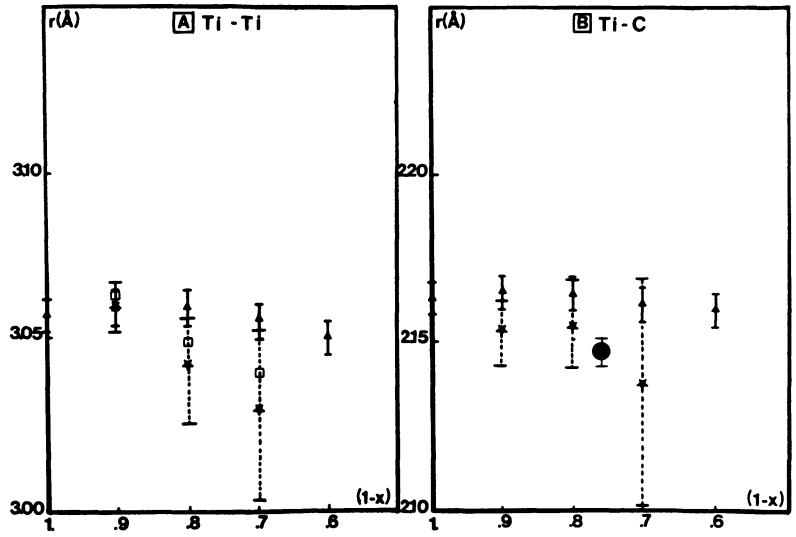


Fig. 7. — Ti-Ti and Ti-C first neighbour average interatomic distances in $TiC_{1-x}$ : (i) from X-ray diffraction measurements (▲) ; (ii) from Exafs determinations using the Gaussian model and phase shifts measured in TiC (★) or interpolated between Ti and TiC (□) ; (iii) from elastic diffuse neutron scattering measurements on $TiC_{0.76}$ (◆) (Ref. [45]).

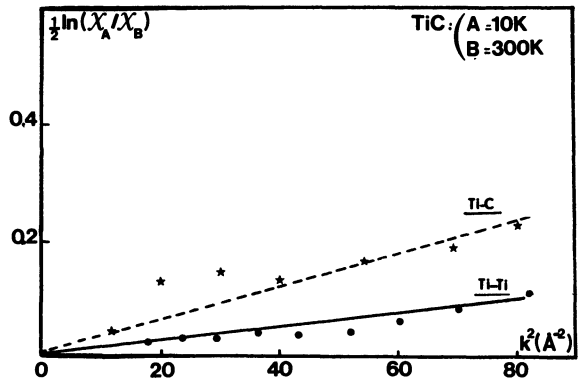


Fig. 8. — $\frac{1}{2}\ln\left(\frac{\chi_A}{\chi_B}\right)$ values measured at the partial Exafs oscillations maxima in TiC *versus* $k^2$: $\chi_A$ and $\chi_B$ correspond respectively to 10 K and 300 K experiments ; (•) and (*) experimental results for Ti-Ti and Ti-C first neighbours ; (------) and (——) linear adjusted functions *versus* $k^2$.

the thermal vibrations in TiC up to 300 K. The fit gives :

$$\sigma^2_{\text{Ti-Ti}}\ (300\ \text{K}) - \sigma^2_{\text{Ti-Ti}}\ (10\ \text{K}) = 0.0013\ (5)\ \text{Å}^2$$
$$\sigma^2_{\text{Ti-C}}\ (300\ \text{K}) - \sigma^2_{\text{Ti-C}}\ (10\ \text{K}) = 0.0030\ (10)\ \text{Å}^2\ .$$

The $\sigma^2_{\text{Ti-Ti}}$ and $\sigma^2_{\text{Ti-C}}$ values deduced from Exafs are smaller than the sum of (*one dimensional*) individual thermal mean square displacements $2\,\sigma'^2_{\text{Ti}}$ and $\sigma'^2_{\text{Ti}} + \sigma'^2_{\text{C}}$ respectively, because the first neighbour movements are partially correlated (in particular, the long wavelength vibrations do not contribute to $\sigma^2_{\text{Ti-Ti}}$). From data of literature [37-39],

$$\sigma'^2_{\text{Ti}}\ (10\ \text{K}) = 0.0013\ \text{Å}^2,\ \sigma'^2_{\text{Ti}}\ (300\ \text{K}) = 0.0023\ \text{Å}^2\ ,$$
$$\sigma'^2_{\text{C}}\ (10\ \text{K}) = 0.0024\ \text{Å}^2,\ \sigma'^2_{\text{C}}\ (300\ \text{K}) = 0.0033\ \text{Å}^2\ .$$

The Exafs thermal Debye-Waller factor has only been discussed for pure metals [36] : the reduction of first neighbour interatomic $\sigma^2$ due to movement correlations varies from about 20 % at 0 K to 40 % above Debye temperature ; our data for $\sigma^2_{\text{Ti-Ti}}$ in TiC are in qualitative agreement with these results.

For non-stoichiometric $TiC_{1-x}$, the same $\sigma^2\ (300\ \text{K}) - \sigma^2\ (10\ \text{K})$ values than for TiC were found (within the error bars).

5.2.3 *Static displacements.* — In the Gaussian model of disorder, the amplitude ratio of the partial Exafs functions relative to the same shell of neighbours in TiC and $TiC_{1-x}$ at a given temperature, may be written as :

$$\ln\left[\frac{\chi_{j\text{A}}(k)}{\chi_{j\text{B}}(k)}\right] = \ln\left[\frac{N_{j\text{A}}\,\overline{R^2_{j\text{B}}}}{N_{j\text{B}}\,\overline{R^2_{j\text{A}}}}\right] + 2(\sigma^2_{j\text{B}} - \sigma^2_{j\text{A}})\,k^2 \quad (6)$$

where $\text{A} \equiv \text{TiC}$, $\text{B} \equiv TiC_{1-x}$.

The slope of experimental $\frac{1}{2}\ln(\chi_A/\chi_B)$ *versus* $k^2$ will give an evaluation of the relative disorder between the atomic structures of TiC and $TiC_{1-x}$, and the extrapolation at $k = 0$ will measure the possible change of the coordination $N_j$.

In figure 9, are shown the $\frac{1}{2}\ln(\chi_A/\chi_B)$ *versus*

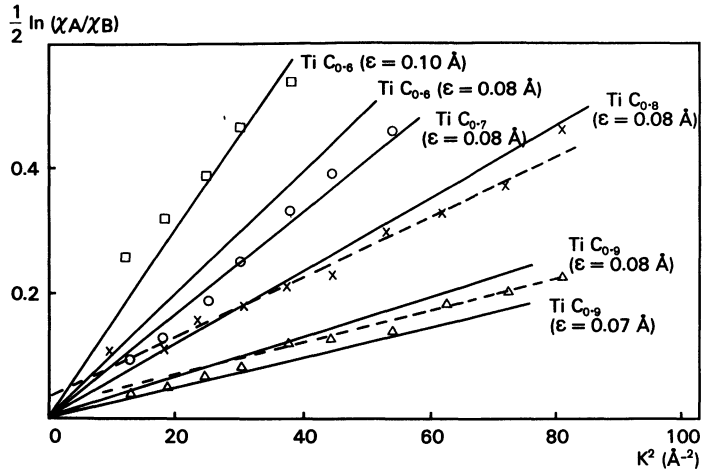


Fig. 9. — $\frac{1}{2}\ln\left(\frac{\chi_A}{\chi_B}\right)$ values measured at the partial Exafs oscillations maxima in $TiC_{1-x}$ *versus* $k^2$ at 10 K : $\chi_A$ and $\chi_B$ correspond respectively to Ti-Ti first neighbours in TiC and $TiC_{1-x}$ : (------) linear fit (Gaussian model) (for $TiC_{0.8}$ and $TiC_{0.9}$) ; (——) fit by the model of section 5.3 with several $\varepsilon$ values. Experimental points : (△) $TiC_{0.9}$ ; (×) $TiC_{0.8}$ (300 K) ; (○) $TiC_{0.7}$ ; (□) $TiC_{0.6}$.

$k^2$ curves for the Ti-Ti first neighbours at 10 K : it is seen that relation (6) is only approximately obeyed. The parameters deduced from the linear fit of these curves in the 4-12 $Å^{-1}$ $k$ range, for the Ti-Ti and Ti-C first neighbours at 10 and 300 K (i.e. relative disorder $\sigma_B^2 - \sigma_A^2$ and coordination $N_B/N_A$) are summarized in figure 10 and table II.

Two statements can be made :

(i) as the thermal contribution $\sigma^2(300\text{ K}) - \sigma^2(10\text{ K})$ was found independent of $x$, $\sigma_{jB}^2 - \sigma_{jA}^2$ can be considered mainly as a static contribution, arising from atomic disorder in $TiC_{1-x}$ : $\sigma_j^{2\,\text{stat.}}$ ; $\sigma_{\text{Ti-Ti}}^{2\,\text{stat.}}$ and $\sigma_{\text{Ti-C}}^{2\,\text{stat.}}$ are found independent of temperature and roughly proportional to the carbon vacancy concentration $x$ for $x \leqslant 0.3$ ;

(ii) the decrease of $N_B/N_A$ for Ti-Ti first neighbours is anomalous, as it should remain equal to 1.

The latter fact, as well as the anomalous apparent decrease of $\overline{R_{\text{Ti-Ti}}}$ (Sect. 5.2.1), suggests that the Gaussian model does not describe correctly the static atomic disorder in $TiC_{1-x}$.

Another defect model is proposed in the following paragraph.

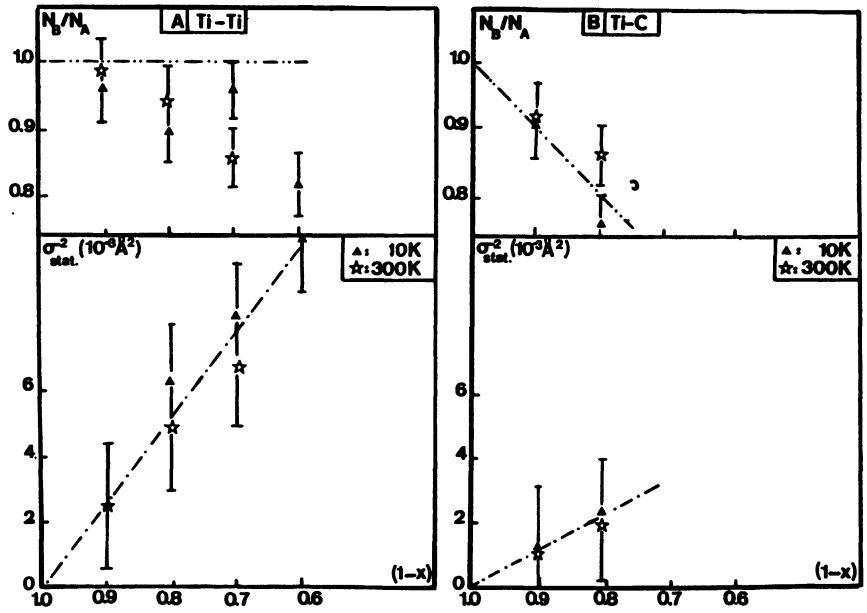


Fig. 10. — Relative coordination and static mean-square displacements variations from TiC to $TiC_{1-x}$ obtained from the Gaussian model fit of Exafs data at 10 and 300 K.

Table II. — *Relative static atomic mean-square displacements of* Ti-Ti *and* Ti-C *first neighbours in* $TiC_{1-x}$, *evaluated from the Gaussian disorder analysis of Exafs data* $\left(\frac{1}{2}\ln(\chi_A/\chi_B)\right.$ *versus* $k^2$ *plots) at* 10 *and* 300 K, *and in the defect model of* section 5.3, *with* $\varepsilon = 0.08$ Å *and* $\delta = 0.04$ Å.

| $TiC_{1-x}$ | $\sigma^2_{Ti\text{-}Ti}$ (Å) | | | $\sigma^2_{Ti\text{-}C}$ (Å) | | |
|---|---|---|---|---|---|---|
| | 10 K Gaussian | 300 K Gaussian | $6x(1-x)\varepsilon^2$ | 10 K Gaussian | 300 K Gaussian | $x(1-x)\varepsilon^2 + 4x\delta^2$ |
| $TiC_{0.9}$ | 0.0025 (10) | 0.0026 (10) | 0.0035 | 0.0012 (10) | 0.0010 (10) | 0.0012 |
| $TiC_{0.8}$ | 0.0063 (20) | 0.0048 (10) | 0.0061 | 0.0023 (10) | 0.0019 (10) | 0.0023 |
| $TiC_{0.7}$ | 0.0083 (15) | 0.0067 (15) | 0.0081 | | | |
| $TiC_{0.6}$ | 0.0114 (15) | | 0.0092 (*) | | | |

(*) 0.0092 in the disordered case, 0.0194 in the ordered case.

5.3 DEFECT STRUCTURE MODEL FOR $TiC_{1-x}$. — Eisenberger and Brown [40] were the first to show that a non-Gaussian asymmetric radial pair distribution function $g(R_j)$ explained the apparent decrease of coordination $N_j$ and average interatomic distances $\overline{R_j}$ in many disordered systems. The model proposed here is based on the crystallographic structures of vacancy-ordered carbides $Ti_2C$, $Zr_2C$, $V_8C_7$, $Nb_6C_5$ [3] where, as shown by X-ray and neutron diffraction, the metal atoms are displaced away from their carbon vacancies first neighbours.

5.3.1 In a first stage, we assumed that the carbon atoms remain (in time average) fixed at their f.c.c. sites, and that each vacancy pushes away radially its six Ti first neighbours by a distance $\varepsilon$. For Ti atoms with several first neighbours vacancies, additivity of the displacement vectors due to each vacancy is assumed. In figure 11 are shown the different possible environments of a Ti-Ti first neighbour pair : it is found that, to first order in $\varepsilon/a$, the corresponding Ti-Ti interatomic distance $R_j$ can take 9 discrete values labelled by the integer index $n = -4$ to $+4$ :

$$R_j = a\sqrt{2}/2 + n\varepsilon\sqrt{2}/2 = a\sqrt{2}/2 + y_n .$$

The static pair distribution function $g_{stat.}(R_j)$ is then a histogram of 9 discrete values $g_n(R_j)$ such that $\sum_{n=-4}^{+4} g_n = 1$. In the case of a random distribution of vacancies and carbon atoms, the expressions for the 9 coefficients $g_n$ are given in table III, and the $g_n$ *versus* $y_n$ histograms are shown in figure 12 : the distribution is found asymmetric except for $x = 0$ and 0.5. One can easily check that $\sum_{n=-4}^{+4} g_n y_n = 0$ (whence $\bar{R}_j = a\sqrt{2}/2$), that the mean-square relative displacement of Ti-Ti first neighbours is

$$\sigma^2_{Ti\text{-}Ti} = \sum_{n=-4}^{+4} g_n (n\varepsilon\sqrt{2}/2)^2 = 6x(1-x)\varepsilon^2$$

and that the individual 3-dimensional Ti mean-square displacement $\sigma^2_{Ti}$ has the same value

$$\sigma^2_{Ti} = 6x(1-x)\varepsilon^2 .$$

Table III. — *Static pair distribution probabilities* $g_n$ *and interatomic distance fluctuations* $y_n$ *for* Ti-Ti *first neighbours in disordered* $TiC_{1-x}$ *in the model described section* 5.3.

| $n$ | $y_n$ | $g_n$ |
|---|---|---|
| $-4$ | $-2\varepsilon\sqrt{2}$ | $x^4(1-x)^2$ |
| $-3$ | $-3\varepsilon\sqrt{2}/2$ | $4x^3(1-x)^3$ |
| $-2$ | $-\varepsilon\sqrt{2}$ | $2x^5(1-x) + 6x^2(1-x)^4$ |
| $-1$ | $-\varepsilon\sqrt{2}/2$ | $8x^4(1-x)^2 + 4x(1-x)^5$ |
| 0 | 0 | $x^6 + 12x^3(1-x)^3 + (1-x)^6$ |
| $+1$ | $+\varepsilon\sqrt{2}/2$ | $4x^5(1-x) + 8x^2(1-x)^4$ |
| $+2$ | $+\varepsilon\sqrt{2}$ | $6x^4(1-x)^2 + 2x(1-x)^5$ |
| $+3$ | $+3\varepsilon\sqrt{2}/2$ | $4x^3(1-x)^3$ |
| $+4$ | $+2\varepsilon\sqrt{2}$ | $x^2(1-x)^4$ |

5.3.2 The partial Exafs $\chi_{Ti\text{-}Ti}(k)$ can then be recalculated exactly using the formalism of Eisenberger and Brown [40] and the above model. The pair distribution function $g(R_j)$ is written

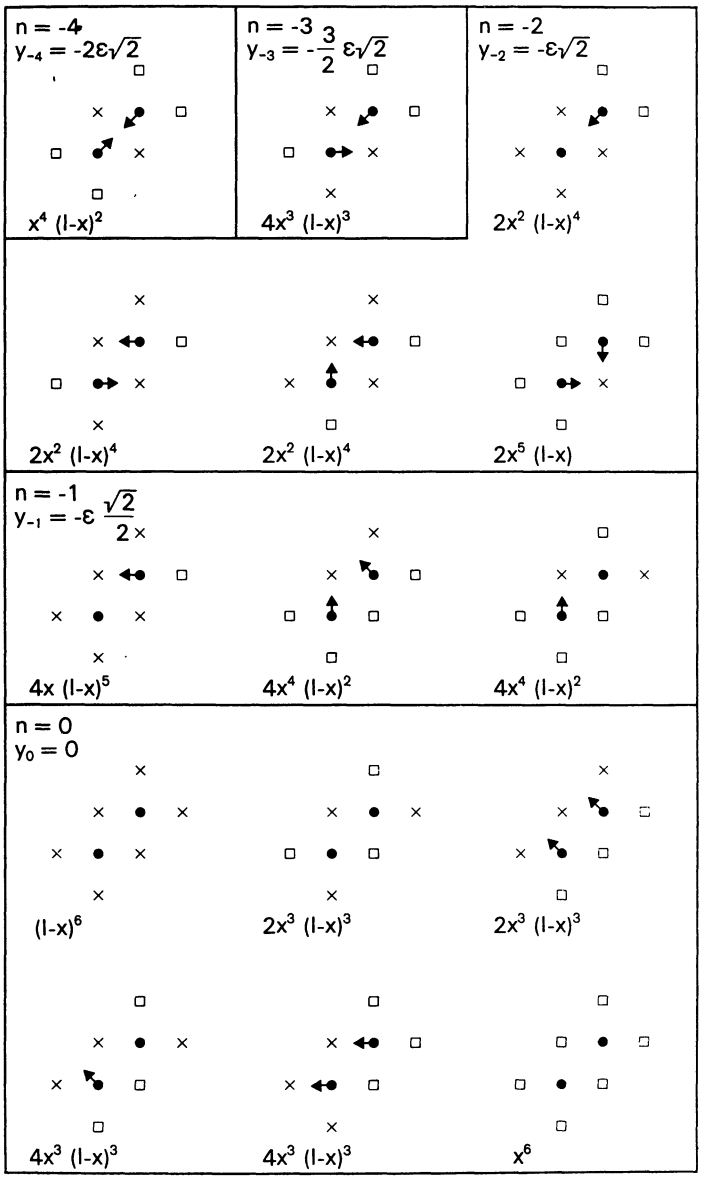


Fig. 11. — Different atomic environments of a Ti-Ti first neighbour pair in the (001) lattice plane of $TiC_{1-x}$, consisting of six sites of the metalloid sublattice. The individual Ti displacements in the model of section 5.3 are indicated by arrows. The four other metalloid first neighbours (out of 001 plane) do not influence the Ti-Ti distance to first order in $\varepsilon/a$. For each type of environment are indicated the index $n$ (see text), the interatomic Ti-Ti static displacement $y_n$ and the probability of this environment for a random distribution of C and vacancies. (•) Ti ; (×) C ; (□) vacancy.

$$e^{-2\sigma^2_{j\,\text{therm.}}k^2} \cdot g_{\text{stat.}}(R_j) ,$$

where $g_{\text{stat.}}$ is given in table III. The integral in equation (1) takes the form :

$$e^{-2\sigma^2_{j\,\text{therm.}}k^2} \frac{1}{\sqrt{A_k^2 + S_k^2}} \times \sin\left(2k\bar{R}_j + \psi_j(k) + \text{Arc tg}\frac{A_k}{S_k}\right) \quad (7)$$

with

$$A_k = \sum_{n=-4}^{+4} g_n \sin 2ky_n ,$$

and

$$S_k = \sum_{n=-4}^{+4} g_n \cos 2ky_n$$

(for $x = 0 : A_k = 0,\ S_k = 1$).

The relative damping between $TiC_{1-x}$ (sample B) and TiC (sample A), $\frac{1}{2}\ln\frac{\chi_A}{\chi_B}$, is given by $\frac{1}{2}\ln\frac{1}{\sqrt{A_k^2 + S_k^2}}$ which is not a linear function of $k^2$.

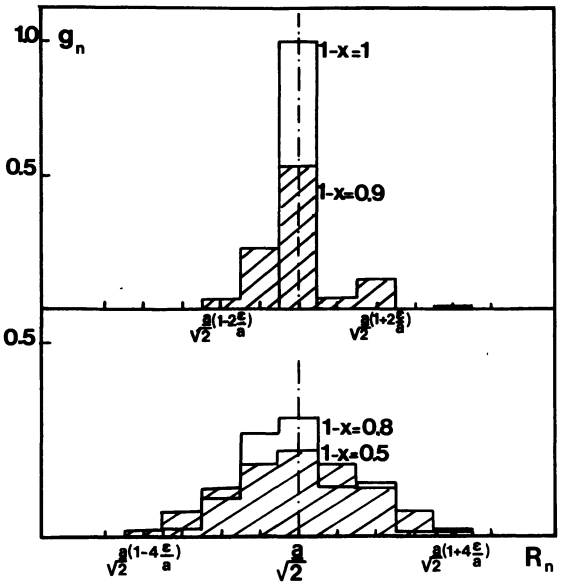


Fig. 12. — Non-Gaussian Ti-Ti first neighbour interatomic distance distribution obtained in the model of section 5.3 for different compositions $TiC_{1-x}$.

• For $0.7 \leqslant 1-x < 1$, vacancies and carbon atoms are taken to be randomly distributed, as elastic neutron diffuse scattering experiments have shown that the short-range order in $TiC_{0.76}$ is weak [35]. The fit to the experimental data $\frac{1}{2} \ln \frac{\chi_A}{\chi_B}$ was then made using the $g_n$ values of table III ; the best fit, shown in figure 9, corresponds to the following $\varepsilon$ values : 0.075 Å for $TiC_{0.9}$, 0.085 for $TiC_{0.8}$ and $TiC_{0.7}$.

• $TiC_{0.6}$ presents a strong tendency for vacancy ordering and must be discussed separately : it can be shown that ordering increases $\sigma^2_{\text{Ti-Ti}}$ for a given $\varepsilon$ ; if one assumes either of the two proposed long-range ordered superstructures for $TiC_{0.5\text{-}0.65}$ ($R\bar{3}m$ type CuPt, or Fd3m [7]), the excess carbon relative to the ideal composition $Ti_2C$ being randomly distributed on the vacancy sublattice, one can calculate that $\sigma^2_{\text{Ti-Ti}} = [6x(1-x) + 10x^2]\,\varepsilon^2$ ; the fit to experimental data gives for $TiC_{0.6}$ : $\varepsilon = 0.07$ Å (instead of 0.10 Å if ordering is neglected).

• These results are obtained neglecting short-range order between carbons and vacancies, and assuming that the thermal displacements are independent of composition. We can show that these two approximations have only small effects on $\varepsilon$. (i) For $0.7 \leqslant 1-x < 1$, short-range order is mainly characterized by a tendency for two vacancies to avoid f.c.c. second neighbour positions, i.e. by a negative Cowley-Warren coefficient $\alpha_{002}$ [35] ; for $TiC_{0.8}$, we recalculated $\sigma^2_{\text{Ti-Ti}}$ after introduction of a short-range order parameter $\alpha_{002} = -0.1$ [45] ; this causes a small modification of $\varepsilon$ : 0.08 instead of 0.085 Å.

(ii) The Ti Debye-Waller factor at 300 K increases with $x$ ; we estimated from various data of literature [36, 37, 39] $\sigma^2_{\text{Ti-Ti therm.}}$ (10 K) $\simeq 0.0021$ Å$^2$ for stoichiometric TiC (see Sect. 5.2.2) ; assuming its variation with $x$ is proportional to that of $\sigma^2_{\text{Ti therm.}}$ (300 K), i.e. an increase of 25 % from TiC to $TiC_{0.8}$ [37], leads to a small decrease of the calculated static Debye-Waller factor and of $\varepsilon$ : 0.0082 instead of 0.0085 Å.

In conclusion, it is reasonable, within the error bars, to take $\varepsilon$ constant in all the $TiC_{1-x}$ composition range, and equal to $0.08 \pm 0.01$ Å. The calculated mean-square relative displacements are given in table II.

5.3.3 For the Ti-C first neighbours, the same model gives (to first order in $\varepsilon/a$) two distances : $a/2$ and $a/2 - \varepsilon$, with respective weights $g'_0 = 1-x$ and $g'_1 = x$. The average distance is then $\overline{R_{\text{Ti-C}}} = a/2 - x\varepsilon$, and the mean square displacement $\sigma^2_{\text{Ti-C}} = x(1-x)\,\varepsilon^2 = \frac{1}{6}\sigma^2_{\text{Ti-Ti}}$. As experimentally one observes $\sigma^2_{\text{Ti-C}} \simeq \frac{1}{2}\sigma^2_{\text{Ti-Ti}}$ (see Tab. II), this means that the carbon atoms are also displaced. We refined the model, assuming that each vacancy displaces also radially its twelve C first neighbours by a distance $\delta$.

This does not change $\overline{R_{\text{Ti-C}}} (= a/2 - x\varepsilon)$, but the mean-square displacement becomes :

$$\sigma^2_{\text{Ti-C}} = x(1-x)\,\varepsilon^2 + 4x\delta^2 .$$

The fit of experimental data (Fig. 9) for $TiC_{0.9}$ and $TiC_{0.8}$ gives then $|\delta| = 0.04 \pm 0.02$ Å.

5.3.4 Formula (7) shows that the asymmetry of the $g_n$ distribution introduces a corrective term $\Sigma_k = \frac{1}{2k}$ Arc tg $(A_k/S_k)$ to the distances $\bar{R}_j$ deduced from the Gaussian formula (4). We calculated $\Sigma_k$ for the Ti-Ti and Ti-C first neighbours using the $\varepsilon$ and $\delta$ values determined above from the damping of the Exafs spectra. It can be shown that the carbon displacements $\delta$ do not contribute to $A_k$ and do not affect the average distances.

For Ti-C pairs in $TiC_{0.8}$ and $TiC_{0.9}$, $\Sigma_k$ is found small and positive ($\leqslant 0.005$ Å) for all the $k$ range studied (4-12 Å$^{-1}$) : the contraction of $\overline{R_{\text{Ti-C}}}$ observed in figure 7 may be considered as intrinsic.

For the Ti-Ti pairs, $\Sigma_k$ is larger, negative and varies with $k$ ; typically, for $TiC_{0.8}$, $\Sigma_k = -0.002$, $-0.010$ and $-0.027$ Å for $k = 4$, 8 and 12 Å$^{-1}$ respectively. This variation with $k$ explains largely the error bars on $\overline{R_{\text{Ti-Ti}}}$ calculated with the Gaussian model ($\pm 0.015$ Å), and the apparent contraction compared to the X-ray data ($-0.011$ Å with phase-shift interpolated between Ti and TiC, close to $-0.010$ Å the $\Sigma_k$ value calculated at the middle of

the $k$ window, i.e. for $k = 8$ Å$^{-1}$). The same agreement is found for $TiC_{0.9}$ and $TiC_{0.7}$.

5.4 DISCUSSION. — The static displacement model proposed in section 5.3 explains satisfactorily the anomalies deduced from a Gaussian analysis, in particular the apparent decrease of Ti-Ti coordination and average distance for non-stoichiometric samples.

It is interesting to compare the obtained results with the criteria given by Eisenberger and Brown [40] for the validity of the Gaussian description (Eq. (4)) to obtain a precision of 0.01 Å in distance evaluation. For Ti-Ti first neighbours in $TiC_{1-x}$, the criteria may be written :

$$\sigma^2_{\text{Ti-Ti}}/\overline{R_{\text{Ti-Ti}}} \leqslant 0.01 \text{ Å} \qquad (8)$$

and

$$8\,k^3\langle y_n^3\rangle = 8\,k^3 \sum_{n=-4}^{+4} g_n(y_n)^3 \ll 1\,. \qquad (9)$$

For $TiC_{0.8}$, (i) $\sigma^2_{\text{Ti-Ti}}/\overline{R_{\text{Ti-Ti}}}$ is found equal to 0.004 Å, including thermal vibrations : criterion (8) is satisfied ; (ii) $8\,k^3\langle y_n^3\rangle = 0.856$ and 2.89 for $k = 8$ and 12 Å$^{-1}$ respectively : we are at the limit of applicability of criterion (9) and therefore of the Gaussian model. In conclusion, it is the asymmetry of the static Ti-Ti distance distribution (and not its width) which is responsible for the non-applicability of equation (4).

The results of the model of section 5.3 are :

- $\varepsilon = 0.08 \pm 0.01$ Å, the titanium atoms being repelled axially from each vacancy (an attraction would give an apparent expansion of $\overline{R_{\text{Ti-Ti}}}$) ;
- $|\delta| \sim 0.04$ Å, but the sign of the carbon displacements could not be determined, and the precision is low due to the weak carbon backscattering amplitude.

The $\varepsilon$ value can be compared to those obtained by other techniques :

(i) elastic neutron diffuse scattering experiments on a $TiC_{0.76}$ single crystal [35, 45] show a *contraction* of the average Ti-C first neighbour distance : $0.016 \pm 0.003$ Å, whence $\varepsilon = 0.067 \pm 0.013$ Å. The diffuse scattering gives the Fourier transform of the displacement field in all the crystal, while the Exafs gives a selected information for the first neighbour shells ;

(ii) channeling experiments were also performed on a $TiC_{0.9}$ single crystal [39]. The carbon displacements were not detected ($< 0.05$ Å). But, using a Gaussian model for disorder, the mean square Ti displacement (relative to the lattice sites) was found independent of temperature and equal to $0.04 \pm 0.01$ Å, whence $\varepsilon = 0.054 \pm 0.015$ Å.

(iii) X-ray diffraction measurements of the valence electron density distribution in a $TiC_{0.94}$ single crystal [38] were analysed by a sophisticated model, incorporating static displacements along [100] of the metal atoms neighbour to a carbon vacancy ; the refinement of data led to a displacement $\varepsilon = 0.097$ (2) Å ;

(iv) the analysis of the thermal dependence of the Ti Debye-Waller factor in $TiC_{0.967}$ [41] allowed to estimate the static contribution, which corresponds to average displacements $\simeq 0.1$ Å of the Ti atoms close to a carbon vacancy ;

(v) the composition dependence of the F peak position observed in Xanes, analysed by the Natoli relation assuming the reference energy $E_{\text{ref}}$ does not change with $x$, led to $\varepsilon = 0.065 \pm 0.02$ Å (see Sect. 4.2.4).

## 6. Conclusion.

The Ti-K Xanes features in TiC show good agreement with the band structure assuming (dipolar unallowed) 1s → 3d transitions in the 8 eV above the Fermi level. A study of the orientation dependence in a single crystal, using the linearly polarized characteristic of synchrotron radiation, might allow to check if quadrupolar transitions are involved. For non-stoichiometric compounds $TiC_{1-x}$, we have observed an increase of the density of states at the Fermi level, a shift of the bottom of the unoccupied Ti 4p bands towards $E_F$, and a decrease of the titanium effective charge. The latter observation is in contrast with available band calculations ; in fact, realistic band calculations, taking into account the true ordered structure, with carbon vacancies *avoiding* second neighbour positions should be performed ; indeed, calculations for various $Ti_2C$ superstructures [4] show that for the CuPt type ($R\bar{3}m$) ordered structure which is observed experimentally in $TiC_{0.50\text{-}0.65}$, the carbon 2p-metal 3d $e_g$ occupied bands have a much sharper density of states curve than in the other cases (including the disordered compound).

The Exafs study has shown that a Gaussian model for static displacements induced by vacancies is insufficiently accurate : the model proposed in section 5.3 allowed us to obtain an exact solution of the Eisenberger and Brown formalism (to first order in $\varepsilon/a$ and $\delta/a$) : it explains satisfactorily the apparent anomalous decrease of Ti-Ti first neighbour coordination and average distance observed in the Gaussian analysis, assuming that each vacancy repels its six Ti first neighbours by 0.08 Å and displaces its 12 carbon first neighbours by $\simeq 0.04$ Å (in fact, elastic neutron diffuse scattering experiments [45] show that the carbons are attracted by their vacancies first neighbours by 0.032 Å).

Some of the experimental observations discussed

here are at the limit of the precision : the difference between interatomic distances obtained from Exafs and X-ray diffraction ($\leqslant 0.03$ Å) and the results concerning the carbon displacements. On the other hand, the $|\varepsilon|$ value deduced from the damping of the very intense first neighbour Ti-Ti partial Exafs is quite precise ; it is somewhat smaller than that found for niobium carbide $NbC_{1-x}$ by channeling [42] and X-ray Debye-Waller [43] measurements : $0.12 \pm 0.01$ Å. The latter experiments and related lattice statics calculations [42-44] confirmed also (i) the quasi-independency of $\varepsilon$ with composition $x$, (ii) the additivity of thermal and static Debye-Waller factors, and (iii) that for $x \gtrsim 0.1$, the metal static Debye-Waller factor is entirely dominated by the large displacements of the first nearest neighbours calculated in a single vacancy model. It is interesting to mention that the X-ray diffraction experiments reported in [43], performed in the range $4 < k < 28$ Å$^{-1}$, have also shown that, contrary to the case of thermal vibrations, the attenuation of integrated diffraction intensities by static displacements cannot be represented by a simple exponential $\exp(-\sigma^2_{Ti} k^2/3)$ (but the X-ray Debye-Waller factor measures the mean-square displacement from the lattice sites $\sigma^2_{Ti}$, whereas Exafs depends of the *interatomic* mean-square displacements $\sigma^2_{Ti\text{-}Ti}$ or $\sigma^2_{Ti\text{-}C}$).

At last, the indications from the present work concerning the sign of $\varepsilon$ (i.e. the first Ti neighbours of a C vacancy move *away* from the vacancy) are summarized below :

— the decrease of average Ti-C first neighbour distance (see Fig. 7) ;

— the sign of the error $\Sigma_k$ on Ti-Ti average distance introduced by the asymmetric $g_{stat.}(R_{Ti\text{-}Ti})$ histogram (see Fig. 12) ;

— the positive shift with increasing non-stoichiometry $x$ of the energy position of the F peak observed in Xanes (see Sect. 4.2), the magnitude of which is in qualitative agreement with the $\varepsilon$ value.

**Acknowledgments.**

The authors wish to sincerely thank Drs P. Lagarde who critically read a first version of the manuscript, B. Poumellec who pointed out to us several references and in particular the Natoli relation, P. Čapkova who communicated to us thermal Debye-Waller factor values for $TiC_{1-x}$, and D. Raoux for previous useful discussions. We also acknowledge Drs. H. Launois who initiated this study, and P. Bondot for participation to the data analysis program. At last, we thank the referees for useful comments.

## References

[1] STORMS, E. K., The refractory carbides (Academic Press, New York) 1967.

[2] TOTH, L. E., Transition Metal Carbides and Nitrides (Academic Press, New York) 1971.

[3] DE NOVION, C. H. and LANDESMAN, J. P., *Pure Appl. Chem.* **57** (1985) 1391.

[4] LANDESMAN, J. P., TREGLIA, G., TURCHI, P. and DUCASTELLE, F., *J. Phys. France* **46** (1985) 1001.

[5] LEE, P. A., CITRIN, P. H., EISENBERGER, P. and KINCAID, B. M., *Rev. Mod. Phys.* **53** (1981) 769.

[6] BALZAROTTI, A., DE CRESCENZI, M. and INCOCCIA, L., *Phys. Rev. B* **25** (1982) 6349.

[7] MOISY-MAURICE, V., LORENZELLI, N., DE NOVION C. H. and CONVERT, P., *Acta Metall.* **30** (1982) 1769.

[8] RAOUX, D., PETIAU, J., BONDOT, P., CALAS, G., FONTAINE, A., LAGARDE, P., LEVITZ, P., LOUPIAS, G. and SADOC, A., *Revue Phys. Appl.* **15** (1980) 1079.

[9] MOISY-MAURICE, V., Note CEA-N-2171, Saclay (1980).

[10] MÜLLER, J. E., JEPSEN, O. and WILKINS, J. W., *Solid State Commun.* **42** (1982) 365.

[11] PFLÜGER, J., FINK, J., CRECELIUS, G., BOHNEN, K. P. and WINTER, H., *Solid State Commun.* **44** (1982) 489.

[12] NECKEL, A., SCHWARZ, K., EIBLER, R., RASTL, P. and WEINBERGER, P., *Mikrochim. Acta (Wien)* **suppl. 6** (1975) 257.

[13] ZHUKOV, V. P. and GUBANOV, V. A., *J. Phys. Chem. Solids* **48** (1987) 187.

[14] SCHWARZ, K., *J. Phys. C* **10** (1977) 195.

[15] NECKEL, A., RASTL, P., EIBLER, R., WEINBERGER, P. and SCHWARZ, K., *J. Phys. C* **9** (1976) 579.

[16] FISHER, D. W., *J. Appl. Phys.* **41** (1970) 3561.

[17] RIEHLE, F., WOLF, Th., and POLITIS, C., *Z. Phys. B* **47** (1982) 201.

[18] POUMELLEC, B., LAGNEL, F., MARUCCO, J. F. and TOUZELIN, B., *Phys. Status Solidi (B)* **133** (1986) 371.

[19] WAKOH, S. and KUBO, Y., Technical Report of the ISSP (University of Tokyo, Japan) 1971.

[20] RAMQVIST, L., *J. Appl. Phys.* **42** (1971) 2113.

[21] WONG, J., LYTTLE, F. W., MESSMER, R. P. and MAYLOTTE, D. H., *Phys. Rev. B* **30** (1984) 5596.

[22] JOHANSSON, L. I., HAGSTROM, A. L., JACOBSON, B. E. and HAGSTROM, S. B. M., *J. Electron. Spectrosc. Relat. Phenom.* **10** (1977) 259.

[23] NECKEL, A., *Int. J. Quantum Chem.* **XXIII** (1983) 1317.
[24] CAUDRON, R., CASTAING, J. and COSTA, P., *Solid State Commun.* **8** (1970) 621.
[25] KLIMA, J., *J. Phys. C* **12** (1979) 3691.
[26] MARKSTEINER, P., WEINBERGER, P. and NECKEL, A., 8th Int. Conf. on Solid Compounds of Transition Elements (Vienna) 9-13 April 1985, paper P2-B7.
[27] REDINGER, J., EIBLER, R., HERZIG, P., NECKEL, A., PODLOUCKY, R. and WIMMER, E., *J. Phys. Chem. Solids* **46** (1985) 383.
[28] GUBANOV, V. A., KURMAEV, E. Z. and ELLIS, D. E., *J. Phys. C* **14** (1981) 5567.
[29] BOUTARD, J. L., DE NOVION, C. H. and ALLOUL, H., *J. Phys. France* **41** (1980) 845.
[30] RAMQVIST, L., HAMRIN, K., JOHANSSON, G., FAHLMAN, A. and NORDLING, C., *J. Phys. Chem. Solids* **30** (1969) 1835.
[31] KUTZLER, F. W. and ELLIS, D. E., *Phys. Rev. B* **29** (1984) 6890.
[32] NATOLI, C. R., Exafs and NES III, Eds. K. O. Hodgson, B. Hedman and J. E. Penner-Hahn, Proc. in Phys. 2 (Springer-Verlag, Berlin) 1984, p. 38.
[33] TEO, B. K. and LEE, P. A., *J. Am. Chem. Soc.* **101** (1979) 2815.
[34] NOGUERA, C. and SPANJAARD, D., *J. Phys. F* **11** (1981) 1133.
[35] MOISY-MAURICE, V., DE NOVION, C. H., CHRISTENSEN, A. N. and JUST, W., *Solid State Commun.* **39** (1981) 661.
[36] SEVILLANO, E., MEUTH, H. and REHR, J. J., *Phys. Rev. B* **20** (1979) 4908.
[37] ČAPKOVA, P., DOBIASOVA, L. and MAIXNER, J., *Phys. Status Solidi (A)* **87** (1985) K 139 ; and ČAPKOVA, P., private communication.
[38] DUNAND, A., FLACK, H. D. and YVON, K., *Phys. Rev. B* **31** (1985) 2299.
[39] KAUFMANN, R. and MEYER, O., *Solid State Commun.* **51** (1984) 539.
[40] EISENBERGER, P. and BROWN, G. S., *Solid State Commun.* **29** (1979) 481.
[41] ČAPKOVA, P., KUZEL, R. and SEDIVY, J., *Phys. Status Solidi (A)* **76** (1983) 383.
[42] KAUFMANN, R. and MEYER, O., *Phys. Rev. B* **28** (1983) 6216.
[43] METZGER, T. H., PEISL, J. and KAUFMANN, R., *J. Phys. F* **13** (1983) 1103.
[44] LESUEUR, D., *J. Nucl. Mater.* **102** (1981) 87.
[45] PRIEM, T., BEUNEU, B. and DE NOVION, C. H., to be published.